Computational Studies on the Reaction Pathways of CF_3Br with $O(^1D,^3P)$ Atoms

Luning Zhang and Qi-zong Qin*

Department of Chemistry, Laser Chemistry Institute, Fudan University, Shanghai 200433, P. R. China

Received: July 18, 2000; In Final Form: October 24, 2000

The triplet and singlet potential energy surfaces (PES) for $O(^3P,^1D) + CF_3Br$ reactions have been studied using the density functional method at the B3LYP level. Geometries, energies, and vibrational frequencies of CF_3Br, CF_3BrO ($^1A'$ and $^3A''$), CF_3OBr ($^1A'$), CF_3, BrO, CF_2O, BrF, and CF_2O-BrF complexes have been examined. Transition states connecting these species have been characterized and the whole potential surfaces could satisfactorily describe the $O + CF_3Br$ reactions. In the gas phase, the OBr radical is the main product on both the singlet and triplet PESs. In a condensed matrix, however, CF_3OBr should be the dominant product generating from the recombination of nascent $CF_3 + OBr$.

1. Introduction

CF_3Br (Halon 1301) has long been used as fire fighting agent and refrigerant, and is believed to contribute significantly to atmospheric bromine.[1] Since CF_3Br does not react with OH radicals, its tropospheric lifetimes is very long (65−77 years).[2] In the stratosphere, CF_3Br can either be photodecomposed or react directly with atomic oxygen to generate ozone-depleting agents such as Br and BrO in the gas phase. The following reactions between oxygen atoms and CF_3Br have been extensively investigated in the gas phase: [3−5]

$$O(^1D) + CF_3Br \rightarrow CF_3 + BrO \quad (1)$$

$$O(^1D) + CF_3Br \rightarrow Br + CF_3O \quad (2)$$

$$O(^1D) + CF_3Br \rightarrow CF_3Br + O(^3P) \quad (3)$$

Thompson and Ravishankara[3] have studied the branching ratio for the reactive loss and quenching of $O(^1D)$ by monitoring the time-resolved VUV atomic resonance fluorescence of $O(^3P)$. Recently, Cronkhite and Wine[4] pointed out that reaction 1 is the dominant one for the competing reactions 1 and 2. Alagia et al.[5] have built a model potential energy surface coupled with their molecular beam scattering experiments for $O(^1D) + CF_3Br$ system. They suggested that BrO in reaction 1 could be formed on a reactive PES with a deep energy well stabilizing CF_3OBr intermediates. However, CF_3OBr has never been observed in the gas phase.

Lorenzen-Schmidt et al.[6] and Minkwitz et al.[7] have successfully isolated CF_3OBr and recorded its IR and Raman spectra in an Ar matrix as well as in pure solid state. Quite recently, our group reinvestigated the IR spectra of CF_3OBr in an Ar matrix,[8] and infrared absorptions at 1249.4, 1204.2, and 1201.9 cm^{-1} were assigned to CF_3OBr with the aid of density functional calculations at the B3LYP/6-31+G(d) level. This work is now completed by detailed quantum chemical MO calculations of the potential energy surface (PES) for reactions between CF_3Br and oxygen (both ^1D and ^3P states). Geometries, energies, vibrational frequencies of reactants, products, reaction intermediates, and transition states (TS) are obtained, and we hope these results will be valuable for better understanding the reaction mechanism of the $CF_3Br + O$ system.

* Corresponding author. Fax: +86-21-65102777, e-mail: qzqin@srcap.stc.sh.cn.

2. Computation Methods

Quantum chemical MO calculations were carried out using Gaussian 98 codes.[9] Initial potential energy surface scan was performed using the B3LYP[10,11] method with the 6-31+G(d) basis set. Stationary points of interests were further optimized using the 6-311+G(d) basis set. Harmonic vibrational frequencies were calculated using analytical second derivatives, and zero point vibrational energies (ZPE) were derived. The number of imaginary frequencies were used to characterize the nature of located structures. The ZPEs and the vibrational frequencies of reaction intermediates and transition states are used without scaling. Single point energy calculations were done with 6-311+G(2df) basis sets using the 6-311+G(d) geometries.

Transition state optimizations were done with the synchronous transit-guided quasi-Newton (STQN) method[12] at the B3LYP/6-311+G(d) level. The program can generate a guess for the transition structure that is midway between the reactant and product, and it then goes on to optimize that starting structure to a first-order saddle point automatically. At all the calculated transition states, vibrational normal modes were analyzed to testify the nature of the saddle point. In some cases, intrinsic reaction coordinate (IRC) calculations were performed to follow the reaction path.

3. Results and Discussion

In section 3.1, we will first discuss the intersystem crossing between the singlet and triplet potential energy surfaces (PESs) of the $O + CF_3Br$ system; then we will describe the PESs in detail. These profiles are shown in Figures 1 and 2. Reaction intermediates and the transition states (TS) are calculated with their energies in Table 1 and geometries in Figures 3 and 4. Finally, we will discuss the vibrational frequencies (Tables 2 and 3) of the reaction intermediates and TS in section 3.2.

3.1. Potential Energy Surfaces. *Energies of O (^3P) and O (^1D).* Before we proceed to discuss the reaction PESs, it is necessary to confirm the veracity of our computation methods. In Table 1, experimental energies[13,14] of some species are included for comparison. We note the energy difference between $O(^3P)$ and $O(^1D)$ is calculated to be 63.4 kcal/mol, which severely deviates from the measured value of 45.4 kcal/mol.[13] This large difference originates from the wrong symmetry of the wave function for the $O(^1D)$ atom in a simple closed-shell

10.1021/jp0025330 CCC: $20.00
Published on Web 12/12/2000

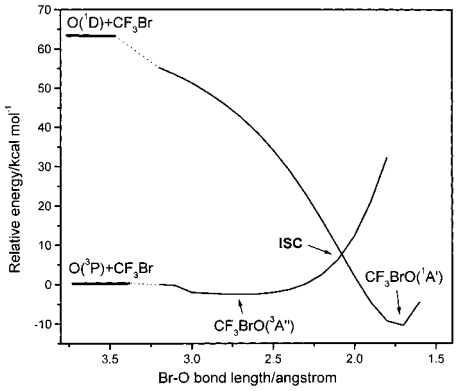

Figure 1. Relative energy of O + CF_3Br interaction on the singlet and triplet PESs plotted as a function of Br−O separation with bent configuration. Calculated at the B3LYP/6-31+G(d) level.

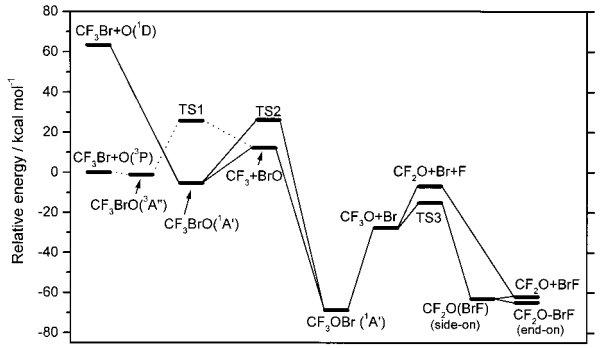

Figure 2. Singlet (solid lines) and triplet (dotted lines) potential energy profiles of the CF_3Br + O system, plotted using B3LYP/6-311+G(d) energies plus ZPE corrections.

TABLE 1: Relative Energies (kcal/mol) of the Reaction Intermediates and Transition States

	energies			
species	6-311+G(d)	6-311+ G(d)+ZPE	6-311+ G(2df)[a]	expt[b]
CF_3OBr ($^1A'$)	−71.36	−68.80	−75.24	
CF_2O−BrF (end on)	−66.34	−64.88	−69.31	
CF_2O(BrF) (side on)	−64.28	−63.08	−67.18	
CF_2O + BrF	−62.88	−62.06	−66.07	
CF_3O + Br	−28.75	−27.78	−28.99	−34.2
CF_2O + Br + F	−6.84	−6.95	−5.26	−10.2
CF_3BrO ($^1A'$)	−6.45	−5.30	−14.04	
CF_3BrO ($^3A''$)	−1.35	−1.13	−1.55	
CF_3Br + O(^3P)	0	0	0	0
CF_3 + BrO	12.53	12.13	8.05	14.0
CF_3Br + O(^1D)	63.36	63.36	63.41	45.45
TS1	25.86	25.68	22.96	
TS2	25.35	26.18	17.47	
TS3	−16.20	−15.28	−17.34	

[a] Single point energy calculated at the B3LYP/6-311+G(d) geometries [b] Relative values of heats of formation ΔH_f (298K). The data are from ref 13, except that of CF_3O, which is from ref 14.

type Kohn−Sham functional. This could be fixed by introducing perfect-pairing general valence bond (GVB-PP) calculation,[9] but unfortunately, it is not available with B3LYP DFT methods.

The singlet−triplet intersystem crossing we are going to discuss is only a qualitative feature, and the aforementioned incorrect energy gap between O(^3P) and O(^1D) will not influence the results. On the other hand, the calculated relative energies accord with experiments with a uncertainty of 2−5 kcal/mol, as shown in Table 1. Therefore, higher level calculations such as CCSD(t) or QCISD have not been performed to correct the energies.

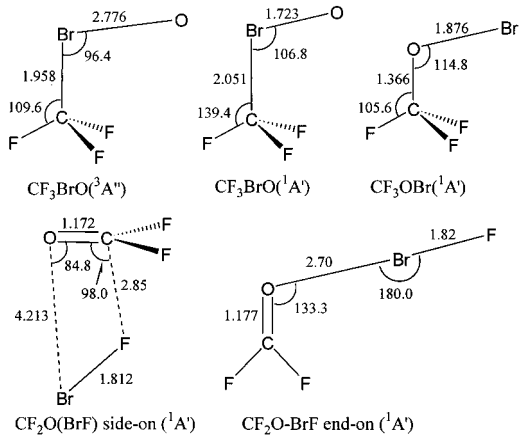

Figure 3. Geometries of CF_3BrO ($^1A'$, $^3A''$), CF_3OBr ($^1A'$), CF_2O-(BrF) side-on complex, and CF_2O−BrF end-on complex. The intermediates all pertain to C_s symmetry.

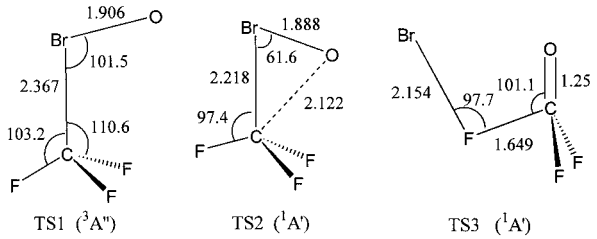

Figure 4. Calculated geometries of the reaction transition states. The TSs all have C_s symmetry.

TABLE 2: Calculated Vibrational Frequencies (cm^{-1}), IR Intensities (in Parentheses, km/mol) of CF_3BrO ($^1A'$, $^3A''$), CF_3OBr, and CF_2O−BrF Complexes at the B3LYP/6-311+G(d) Level

$CF_3BrO(^1A')$	$CF_3BrO(^3A'')$	$CF_3OBr(^1A')$	CF_2O(BrF)(side)	CF_2O−BrF(end)
1224.1 (317)	1188.9 (312)	1214.0 (327)	1970.7 (485)	1937.1 (772)
1210.2 (291)	1180.1 (278)	1185.1 (667)	1205.5 (455)	1245.7 (447)
1043.7 (482)	1047.0 (597)	1163.3 (386)	956.8 (61)	975.0 (66)
735.9 (50)	750.2 (57)	899.2 (6)	768.2 (58)	775.9 (40)
696.0 (43)	541.7 (1)	719.2 (1)	642.8 (35)	627.1 (64)
542.9 (0)	541.5 (1)	644.9 (3)	615.4 (6)	624.6 (11)
525.6 (2)	332.4 (1)	599.8 (3)	576.3 (5)	580.7 (5)
318.6 (3)	297.3 (0)	518.0 (1)	90.7 (2)	124.6 (3)
262.3 (0)	296.4 (0)	423.7 (0)	63.4 (2)	120.1 (2)
249.1 (1)	104.5 (7)	337.3 (3)	50.3 (1)	90.9 (6)
138.8 (8)	27.7 (0)	169.5 (1)	36.9 (1)	47.6 (0)
31.8 (9)	15.7 (0)	88.0 (1)	34.1 (1)	37.8 (0)

TABLE 3: Calculated Vibrational Frequencies (cm^{-1}) of the Reaction Transition States at the B3LYP/6-311+G(d) Level

TS1 $CF_3BrO(^3A'') \rightarrow$ CF_3 + BrO	TS2 CF_3BrO ($^1A'$) → CF_3OBr ($^1A'$)	TS3 CF_3OBr ($^1A'$) → CF_2O(BrF) (side on)
480.3 i	437.1 i	757.8 i
63.7	94.3	34.9
150.6	261.6	239.5
168.1	301.2	284.8
241.8	332.2	316.5
287.3	536.3	479.4
518.3	563.5	586.0
518.8	585.1	604.1
679.4	708.5	705.6
972.5	904.2	941.9
1218.2	1139.8	1193.1
1226.2	1326.2	1429.0

Intersystem Crossing. To characterize the seam of crossing, we scanned the PES for interaction between O(^1D,^3P) and CF_3-Br at the B3LYP/6-31+G(d) level. Previous calculations[15,16] showed that O approaching CF_3I and CH_3I in a bent configu-

ration is energetically favored. Similarly, both singlet and triplet CF_3BrO complexes have bent geometries; therefore we have only calculated the energy along the bent collision trajectories.

As shown in Figure 1, energies along the interaction path are plotted as a function of CF_3Br-O separation. During optimization, we kept the CF_3Br part unchanged, and varied the Br−O bond length. The O atom approaches the Br side in CF_3Br with a C−Br−O angle of 106.8°, the same angle as in the CF_3BrO adducts. As seen from Figure 1, the ISC occurs at a Br−O distance of about 2.1 Å, which is midway between CF_3BrO ($^3A''$) and CF_3BrO ($^1A'$). The crossing point is 2.7 kcal/mol above the O(^3P) + CF_3Br reactants, and also 5.1 and 12.6 kcal/mol higher than the CF_3BrO ($^3A''$) and CF_3BrO ($^1A'$), respectively. The energy of CF_3BrO ($^1A'$) depends significantly on the basis set, as can be seen in Table 1. This implies that the ISC point would also move when using a better basis set. Since the level of theory employed here is below that used to calculate the whole PESs, this picture for ISC is expected to be qualitatively correct.

Previous calculations on the reactions between O (^3P) and CF_3I,[15] CH_3I,[16] and C_2H_5I[17] have shown that the singlet−triplet PES intersections are also important features. As far as we know, the ISC for the CF_3Br + O system is similar to that of the C_2H_5I + O (^1D,^3P) system,[17] of which the ISC occurs at the exit of the entrance valley on the PES.

CF_3BrO and CF_3OBr. The overall potential energy surfaces are given in Figure 2. Starting from O(^3P) and CF_3Br, a vdW complex CF_3BrO ($^3A''$) is located with a binding energy of 1.1 kcal/mol (B3LYP/ 6-311+G(d) + ZPE). Interaction between O(^1D) and CF_3Br leads directly to CF_3BrO ($^1A'$), which is stabilized by about 68 kcal/mol with respect to O(^1D) + CF_3Br. Singlet CF_3BrO ($^1A'$) is a true covalently bound molecule, and it is 5.1 kcal/mol lower in energy than CF_3BrO ($^3A''$). As can be seen from Figure 3, the Br−O bond length in CF_3BrO ($^3A''$) is 2.776 Å, indicating a weak interaction. When it comes to CF_3BrO ($^1A'$), the Br−O bond length becomes 1.723 Å, which is even shorter than that in OBr (1.756 Å), and the C−Br is enlarged to 2.051 Å from 1.948 Å in free CF_3Br. Mulliken population reveals that the BrO bond in CF_3BrO ($^1A'$) is ionic in nature with +0.578 atomic charge on Br and −0.497 on O. This may arise from the donation of the bromine lone pair electrons to the vacant p orbital on oxygen.

Dissociation of CF_3BrO ($^3A''$) to doublet CF_3 + BrO proceeds via TS1, a transition state lying 24.5 kcal/mol above the minimum CF_3BrO ($^3A''$) and 13.6 kcal/mol above CF_3 + BrO. On the singlet surface, CF_3BrO ($^1A'$) generated from O(^1D) + CF_3Br is initially excited by nearly 70 kcal/mol in energy. This molecule can undergo further dissociation/isomerization pathways on the PES, as shown in Figure 2. First, dissociation of CF_3BrO ($^1A'$) by C−Br bond fission to form CF_3 + OBr has no distinct barrier, and the process needs only 18 kcal/mol energy input. Previous experiment[4] found that BrO formation via reaction 1 is the dominant channel with a branching ratio of 0.49 at 298 K. This result accords with our PES qualitatively. Second, CF_3BrO ($^1A'$) could also isomerize through TS2 to form CF_3OBr. This three-center TS lies 31.5 kcal/mol above CF_3-BrO ($^1A'$). However, in comparison with the dissociation channel leading to CF_3 + BrO, this isomerization process is less energetically favored. The geometric parameters of TS1 and TS2 are given in Figure 4.

At the present stage, it is of interest to discuss the origin of CF_3OBr in the matrix isolation experiment.[6,8] Lorenzen-Schmidt et al.[6] have addressed that CF_3OBr came from photodecomposition of the CF_3Br-O_3 complex, and the process is predominantly an insertion reaction. They suggested that direct insertion mechanism should apply or else the byproduct like O_2 might compete with CF_3 and BrO to give CF_3OO or other products. However, under our matrix isolation experiment conditions,[8] the reaction precursors (CF_3Br and O_3) were in good isolation and the product CF_3OBr resulted from separate O(^1D) and CF_3-Br pairs, so the competing pathways involving O_2 can be totally excluded. Accordingly, it is reasonable to recognize that interaction between O(^1D) and CF_3Br leads to CF_3BrO adduct, which readily dissociates to CF_3 and BrO, and fast recombination of nascent CF_3 and BrO leads to CF_3OBr formation.

A dissociation/recombination mechanism for O_3 and CF_3Br reactions in matrix can be proposed as follows:

$$O_3 + h\nu \rightarrow O^*(^1D) + O_2(^1\Delta_g) \text{ (in cage)}$$

$$O^*(^1D) \rightarrow O(^1D) \text{ (cage escape and migration)}$$

$$O(^1D) + CF_3Br \rightarrow CF_3BrO \text{ (addition)}$$

$$CF_3BrO \rightarrow CF_3 + OBr \text{ (dissociation, fast)}$$

$$CF_3 + OBr \rightarrow CF_3OBr \text{ (recombination, fast)}$$

This mechanism can satisfactorily explain the reaction products observed in matrix IR spectra. Moreover, it also supports the gas-phase experiments.[3−5]

Final Product: CF_2O Formation. Now we will concentrate on the latter region of the PES where the final products CF_2O and BrF were produced from O(^1D) + CF_3Br [6,8] reactions. This channel is important in condensed phase reaction,[6,8] although it is not observed in gas phase.

Obviously, CF_2O should come directly from CF_3OBr or CF_3O in which O binds directly with C. We will consider CF_3O first. About 41 kcal/mol energy input is required to break the O−Br bond in CF_3OBr to form CF_3O + Br. Since minor amounts of CF_2O + BrF were observed in matrix isolation experiments,[6,8] it seems a small fraction of initially excited CF_3OBr could still dissociate to CF_3O + Br. One possible channel is that CF_2O + BrF could originate from the following steps: dissociation of CF_3O to CF_2O + F, followed by F atom recombination with Br in a matrix cage forming BrF finally. Normally, C−F bonds are very strong, but it is interesting to notice that the third C−F bond in CF_3O is much weaker than the other two. B3LYP/6-311+G(d) calculations predict its bond energy to be only 21 kcal/mol, much lower than the normal C−F bond strength of 110−120 kcal/mol.

Another possible channel is Br abstraction of F in CF_3O to form a side-on CF_2O(BrF) complex. We have explored the PES and found a transition state (TS3) for this Br abstraction channel:

$$Br + CF_3O \rightarrow TS3 \rightarrow CF_2O(BrF)$$

Figure 4 gives the structure of TS3. In this transition state, the F atom (abstracted by Br) is 1.649 Å away from the C atom, which is 0.32 Å longer than normal C−F bond. The Br−F distance is 2.154 Å, still 0.3 Å away from the free BrF molecule (1.809 Å). TS3 is 12.5 kcal/mol above CF_3O + Br. The final product of this channel is a side-on complex, CF_2O(BrF), which is 1.0 kcal/mol more stable than separated CF_2O + BrF. Geometries of CF_2O(BrF) complexes can be found in Figure 3.

The unimolecular dissociation of CF_3OBr to form the CF_2O-BrF complex is another reaction pathway generating CF_2O. Breaking the C−F and O−Br bonds in CF_3OBr requires lots of energy input. The C−F bond in CF_3OBr should not be as weak as that in CF_3O (vide supra), although it is hard to determine the C−F bond strength here. On that basis, a TS which looks like CF_2OBr with a separate F atom attacking at Br must be high in energy on the PES. Several attempts trying to locate this TS connecting CF_3OBr and $CF_2O(BrF)$ (side-on complex) eventually failed. Thus, we could not judge for the present time whether this unimolecular reaction is applicable, and whether there is a TS for this reaction.

There are two conformers of CF_2O-BrF complexes, namely, side-on and end-on, whose structures are shown in Figure 3. The side-on complex is 1 kcal/mol more stable than separated $CF_2O + BrF$, and the Br−F unit in this complex is parallel to the CF_2O planar with Br interacting with O atom and F with central C atom. The end-on complex has a planar structure with terminal O atom linking Br−F through the bromine atom. The end-on complex is 3 kcal/mol lower in energy than isolated $CF_2O + BrF$. Both complexes have been observed in matrix isolation experiment.[6]

3.2. Vibrational Frequencies. Minkwitz et al. have reported the results of MP2/6-31G* and HF/6-311G* calculations on CF_3OBr.[7] Recently, Kwon et al.[18] calculated the structure, rotational barrier and vibrational frequencies of CF_3OBr using B3LYP method. In our previous study on the IR frequencies of CF_3OBr,[8] we have already carried out B3LYP/6-31+G(d) calculations on both CF_3OBr and CF_3BrO. In this paper, we have completed the previous study with higher level calculations on CF_3OBr and CF_3BrO (both singlet and triplet states). Moreover, final products such as CF_2O-BrF complexes and transition states were also calculated. Vibrational frequencies of these reaction intermediates and TSs are compiled in Tables 2 and 3.

For singlet CF_3BrO ($^1A'$), the most intense bands are two CF_3 asymmetric stretch (1224.1, 1210.2 cm^{-1}) and one CF_3 symmetric stretch (1043.7 cm^{-1}). These modes are close to the corresponding vibrations in CF_3 radical at 1223.0, 1222.9, and 1062.5 cm^{-1}, suggesting a weak C−Br bond in CF_3BrO ($^1A'$). The B3LYP/6-311+G(d) results show that the C−Br bond in CF_3BrO ($^1A'$) is only 18 kcal/mol in strength, much lower than 70.6 kcal/mol in CF_3Br.[19] For triplet CF_3BrO ($^3A''$), the three CF_3 stretch modes are also the most intense absorptions. However, these frequencies are very close to the corresponding modes in free CF_3Br which are 1055.3, 1174.4, and 1174.4 cm^{-1}. This implies that the interaction between CF_3Br and O in CF_3BrO ($^3A''$) is quite weak.

Calculated vibrational frequencies of $CF_3OBr(^1A')$ can reproduce our measured matrix isolation IR spectra[8] very well. B3LYP/6-311+G(d) calculations give three CF_3 stretch frequencies at 1214.0, 1185.1, and 1163.3 cm^{-1}, slightly lower than the experimental values of 1249.4, 1204.2, and 1201.9 cm^{-1}. For the final products of CF_2O and its complexes with BrF, we also found a good match between theoretical and experimental results. Calculated C−O stretch frequencies in CF_2O, $CF_2O(BrF)$ (side on), and CF_2O-BrF (end on) molecules are at 1974.3, 1970.7, and 1937.1 cm^{-1}, respectively. The values and the trend are also in good agreement with measured bands at 1913.3, 1912.5, and 1887.3 cm^{-1}.[6]

4. Conclusion

Singlet and triplet potential energy surfaces for $O(^3P,^1D) + CF_3Br$ reaction pathways have been thoroughly explored by DFT method at B3LYP/6-311+G(d) level. Our calculations show that interaction of $O(^3P)$ with CF_3Br results in CF_3BrO ($^3A''$) formation directly, followed by dissociation to $CF_3 + BrO$ via TS1. On the singlet PES, $O(^1D)$ and CF_3Br interaction leads to CF_3BrO ($^1A'$), and subsequent dissociation of this intermediate to form $CF_3 + BrO$ is barrierless. Singlet−triplet intersystem crossing (ISC) is midway between CF_3BrO ($^3A''$) and CF_3BrO ($^1A'$) at the entrance channel on the PESs. The singlet adduct CF_3BrO ($^1A'$) could further isomerize via TS2 to form CF_3OBr. Initially excited CF_3OBr easily dissociates to $CF_3O + Br$. Since the third C−F bond in CF_3O is calculated to be very weak, we believe either fission of the C−F bond or Br attacking on the F atom (via TS3) would both generate CF_2O, a final product observed in matrix isolation experiments. The PESs obtained in this study can qualitatively explain the complicated behavior of $O + CF_3Br$ reactions.

Acknowledgment. The authors appreciate Dr. Paul Marshall's suggestions on the latter region of the PES. Thanks to Dr. Wang Xuefeng for doing preliminary calculations and Prof. Zheng Qike for fruitful discussion. This work was supported by the Climbing Project of China.

Supporting Information Available: Tables of atomic coordinates. This material is available free of charge via the Internet at http://pubs.acs.org.

References and Notes

(1) Molina, M. J.; Molina, L. T.; Kolb, C. K. *Annu. Rev. Phys. Chem.* **1996**, *47*, 327.

(2) Butler, J. H.; Elkins, J. W.; Hail, B. D.; Cummings, S. O.; Montzka, S. S. *Nature* **1992**, *359*, 403.

(3) Thompson, J. E.; Ravishankara, A. R. *Int. J. Chem. Kinet.* **1993**, *25*, 479.

(4) Cronkhite, J. M.; Wine, P. H. *Int. J. Chem. Kinet.* **1998**, *30*, 555.

(5) Alagia, M.; Balucani, N.; Casavecchia, P.; Lagana, A.; Ochoa de Aspuru, G.; Van Kleef, E. H.; Volpi, G. G.; Lendvay, G. *Chem. Phys. Lett.* **1996**, *258*, 323.

(6) Lorenzen-Schmidt, H.; Weller, R.; Schrems, O. *J. Mol. Struct.* **1995**, *349*, 333.

(7) Minkwitz, R.; Brochler, R.; Kornath, A.; Ludwig, R.; Rittner, F. *Inorg. Chem.* **1997**, *36*, 2174.

(8) Zhang, L.; Wang, X.; Chen, M.; Qin, Q. *Chem. Phys.* **1999**, *249*, 161.

(9) Frisch, M. J.; Trucks, G. W.; Schlegel, H. B.; Scuseria, G. E.; Robb, M. A.; Cheeseman, J. R.; Zakrzewski, V. G.; Montgomery, Jr., J. A.; Stratmann, R. E.; Burant, J. C.; Dapprich, S.; Millam, J. M.; Daniels, A. D.; Kudin, K. N.; Strain, M. C.; Farkas, O.; Tomasi, J.; Barone, V.; Cossi, M.; Cammi, R.; Mennucci, B.; Pomelli, C.; Adamo, C.; Clifford, S.; Ochterski, J.; Petersson, G. A.; Ayala, P. Y.; Cui, Q.; Morokuma, K.; Malick, D. K.; Rabuck, A. D.; Raghavachari, K.; Foresman, J. B.; Cioslowski, J.; Ortiz, J. V.; Baboul, A. G.; Stefanov, B. B.; Liu, G.; Liashenko, A.; Piskorz, P.; Komaromi, I.; Gomperts, R.; Martin, R. L.; Fox, D. J.; Keith, T.; Al-Laham, M. A.; Peng, C. Y.; Nanayakkara, A.; Gonzalez, C.; Challacombe, M.; Gill, P. M. W.; Johnson, B.; Chen, W.; Wong, M. W.; Andres, J. L.; Gonzalez, C.; Head-Gordon, M.; Replogle, E. S.; Pople, J. A. *Gaussian 98*, Revision A.7; Gaussian, Inc.: Pittsburgh, PA, **1998**.

(10) Becke, A. D. *J. Chem. Phys.* **1993**, *98*, 5648.

(11) Lee, C.; Yang, W.; Parr, R. G. *Phys. Rev. B* **1988**, *41*, 485.

(12) Peng, C.; Ayala, P. Y.; Schlegel, H. B.; Frisch, M. J. *J. Comput. Chem.* **1996**, *17*, 49.

(13) Atkinson, R.; Baulch, D. L.; Cox, R. A.; Hampton, R. F., Jr.; Troe, J. A. *J. Phys. Chem. Ref. Data* **1992**, *21*, 1125.

(14) Batt, L.; Walsh, R. *Int. J. Chem. Kinet.* **1982**, *14*, 933.

(15) Wells, D. D.; Mohr, S.; Goonan, K. M.; Hammer, M.; Grice, R. J. *Phys. Chem. A* **1997**, *101*, 7499.

(16) Misra, A.; Berry, R. J.; Marshall, P. *J. Phys. Chem. A* **1997**, *101*, 7420.

(17) Stevens, J. E.; Cui, Q.; Morokuma, K. J. *Chem. Phys.* **1998**, *108*, 1544.

(18) Kwon, O.; Kwon, Y. *THEOCHEM* **1999**, *489*, 119.

(19) Weast, R. C., Astle, M. J., Eds. *CRC Handbook of Chemistry and Physics*, 63rd ed.; CRC Press: Boca Raton, FL, 1982.